This full text paper was peer reviewed at the direction of IEEE Communications Society subject matter experts for publication in the IEEE Globecom 2011 proceedings.

Optimum Sampling in a Spatial-Temporally Correlated Wireless Sensor Network

Ning Sun and Jingxian Wu
Department of Electrical Engineering,
University of Arkansas, Fayetteville, AR 72701, USA.

***Abstract*—The optimum space and time sampling in a wireless sensor network (WSN) with spatial-temporally correlated data is studied in this paper. The impacts of the node density in the space domain and the sampling rate in the time domain on the network performance are investigated asymptotically by considering a large network with infinite area, infinite time period, but finite node density and finite temporal sampling rate. Two cases are studied under the constraint of fixed power per unit area. The first case investigates the estimations of the space-time samples collected by the sensors, and the samples are discrete in both the space and time domains. The second case estimates an arbitrary data point on the space-time plane, by interpolating the discrete samples collected by the sensors. The interactions among the various network parameters and their impacts on the system performance are quantitatively identified with exact analytical expressions.**

I. Introduction

Data collected by a wireless sensor network (WSN) often contain redundancy due to the spatial and temporal correlations inherent in the monitored object(s). The space-time redundancy/correlation is important to the performance and design of practical WSNs. Given a fixed transmission power per unit area, a higher spatial node density or temporal sampling rate means less transmission energy per sample, but more data samples per unit area per unit time. Therefore, it is critical to identify the optimum spatial node density and temporal sampling rate in a spatial-temporally correlated WSN.

The impacts of spatial node density on the network performance have been studied extensively in the literature [1] – [3]. Most of these works only focus on the spatial data correlation and do not consider the variation of the data in the time domain. In reality, the physical phenomenon under monitoring changes with respect to time, and this determines the temporal correlation between the collected samples [4].

There are limited works on the study of WSNs with spatial-temporally correlated data [5] – [8]. In [5] and [6], an arbitrary point on a continuous measurement field is estimated by interpolating the samples collected by the spatially discrete sensors. The studies in [5] and [6] only utilize the temporal data correlation to perform the time domain interpolation, and they do not consider the effects of the temporal sampling rate. The effects of both the space and time domain sampling are studied in [7] by using the network energy as a performance metric, through the study of a collision free network protocol. All of the aforementioned works consider an error-free communication channel between the transmitter and the receiver. The impacts of channel noise are considered in [8]. However, the analysis is only applicable to a measurement field with finite degree-of-freedom and discrete in the time domain. In addition, [8] does not consider the optimum sampling rate in the time domain.

In this paper, we investigate the optimum spatial node density and temporal sampling rate for a WSN with the spatial-temporally correlated data. The fusion center (FC) attempts to reconstruct the continuous data field from the discrete sensor samples transmitted to the FC through a *noisy* link, by exploiting the spatial-temporal correlation with the minimum mean square error (MMSE) receiver. The impacts of the spatial node density, the temporal sampling rate, and the space-time data correlation, on the reconstruction mean square error (MSE) are investigated asymptotically in a large network with infinite area, infinite time period, but finite node density and finite temporal sampling rate. Under the constraint of fixed transmission power per unit area, exact analytical expressions are obtained to describe the interactions and tradeoff relationships between the signal-to-noise ratio (SNR) per sample and the spatial-temporal sample correlation. The optimum spatial-temporal sampling for two types of networks, one needs to recover only the discrete space-time samples, and one needs to recover the data at an arbitrary point on the space-time plane, are identified through the asymptotic analysis.

II. Problem Formulation

A. System Model

Consider a WSN with N_s sensor nodes uniformly placed over a linear measurement field. Data collected from this field are spatially correlated, and they change with respect to time. Each sensor node will measure a spatial-temporally dependent physical quantity, such as the vibration density of a bridge, or the pH value in soil, etc. Let $x(\boldsymbol{\eta})$ represent a data sample of the measurement filed in the two-dimensional (2D) space-time plane, where $\boldsymbol{\eta} = [l, t]$ is the space-time coordinate, with l being the coordinate in the space domain, and t the time instant that the sample is collected.

It is assumed that the physical quantities to be measured form a random process that is wide-sense stationary (WSS) in both the space and time domains. The spatial-temporal correlation function between any two arbitrary data samples is assumed to

This full text paper was peer reviewed at the direction of IEEE Communications Society subject matter experts for publication in the IEEE Globecom 2011 proceedings.

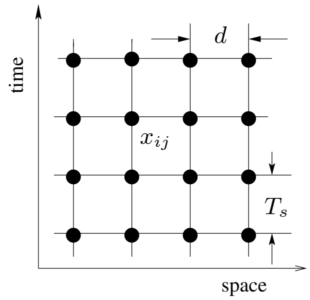

Fig. 1. Space-time samples collected by the WSN.

be

$$\mathbb{E}\left[x(l_1,t_1)x(l_2,t_2)\right] = \rho_s^{|l_1-l_2|}\rho_t^{|t_1-t_2|} \tag{1}$$

where $\rho_s \in [0,1]$ and $\rho_t \in [0,1]$ are defined as the spatial correlation coefficient and the temporal correlation coefficient, respectively, and $\mathbb{E}(\cdot)$ represents mathematical expectation.

As shown in Fig. 1, the system has a spatial node density of $\delta = \frac{1}{d}$, and each sensor node collects N_t data samples with a rate of $\theta = \frac{1}{T_s}$Hz. The j-th data sample collected by the i-th sensor is denoted as $x_{ij} = x(id, jT_s)$.

Define the space-time data sample vector as $\mathbf{x} = [\mathbf{x}_0^T, \cdots, \mathbf{x}_{N_s-1}^T]^T \in \mathcal{R}^{N\times 1}$, where $N = N_s \times N_t$, $\mathbf{A}^T$ represents matrix transpose, $\mathcal{R}$ is the set of real numbers, and $\mathbf{x}_i = [x_{i0}, \cdots, x_{i(N_t-1)}]^T \in \mathcal{R}^{N_t\times 1}$ is the time domain sample vector collected by the i-th sensor node. The spatial-temporal correlation matrix, $\mathbf{R}_{xx} = \mathbb{E}\left[\mathbf{x}\mathbf{x}^T\right] \in \mathcal{R}^{N\times N}$, can then be expressed as

$$\mathbf{R}_{xx} = \mathbf{R}_s \otimes \mathbf{R}_t \tag{2}$$

where $\otimes$ is the Kronecker product operator, and $\mathbf{R}_s \in \mathcal{R}^{N_s\times N_s}$ and $\mathbf{R}_t \in \mathcal{R}^{N_t\times N_t}$ are the correlation matrices in the space and time domains, respectively. The matrix, $\mathbf{R}_s$, has the form of a symmetric Toeplitz matrix with the first row and first column being $\mathbf{r}_s = \left[1, \rho_s^d, \cdots, \rho_s^{(N_s-1)d}\right]^T$. Similarly, the matrix, $\mathbf{R}_t$, is a symmetric Toeplitz matrix with the first row and first column being $\mathbf{r}_t = \left[1, \rho_t^{T_s}, \cdots, \rho_t^{(N_t-1)T_s}\right]^T$. The matrix $\mathbf{R}_{xx}$ has the form of a Toeplitz-block-Toeplitz (TBT) matrix [9].

It is assumed that sensors deliver the measured data to the FC through an orthogonal media access control (MAC) scheme, such as the deterministic frequency division multiple access (FDMA), such that collision-free communication is achieved at the FC. The signal observed by the FC from the j-th time sample of the i-th sensor node is

$$y_{ij} = \sqrt{E_{ij}} \cdot x_{ij} + z_{ij}, \tag{3}$$

where E_{ij} is the average transmission energy per sample, and z_{ij} is the additive white Gaussian noise (AWGN) with variance σ_z^2. The system model does not consider the effects of fading or pathloss. The subsequent analysis can be easily extended to systems with fading. It is assumed that the total power per unit area is fixed at P_0. Given a network with a node density δ and a sample rate θ, the transmission energy per sample can be written as $E_{ij} = \frac{P_0}{\theta\delta}$.

B. Optimum MMSE Detection

The FC will obtain an estimate of the spatial-temporally continuous quantity, $x(\boldsymbol{\eta})$, $\forall \boldsymbol{\eta} \in \Omega_{\boldsymbol{\eta}}$, where $\Omega_{\boldsymbol{\eta}}$ is the 2D space-time plane, by using the N discrete space-time samples received at the FC, $\mathbf{y} = [\mathbf{y}_0^T, \cdots, \mathbf{y}_{N_s-1}^T]^T \in \mathcal{R}^{N\times 1}$, where $\mathbf{y}_m = [y_{m0}, \cdots, y_{m(N_t-1)}]^T \in \mathcal{R}^{N_t\times 1}$. The MSE for $x(\boldsymbol{\eta})$ is

$$\sigma_{\boldsymbol{\eta}}^2 = \mathbb{E}\left[\hat{x}(\boldsymbol{\eta}) - x(\boldsymbol{\eta})\right]^2, \boldsymbol{\eta} \in \Omega_{\boldsymbol{\eta}} \tag{4}$$

where $\hat{x}(\boldsymbol{\eta})$ is the estimate of $x(\boldsymbol{\eta})$ at the FC.

The optimum linear receiver that minimizes $\sigma_{\boldsymbol{\eta}}^2$ is the MMSE receiver described as follows [10]

$$\hat{x}(\boldsymbol{\eta}) = \sqrt{E_{ij}}\mathbf{r}_{\boldsymbol{\eta}}^T\left(E_{ij}\mathbf{R}_{xx} + \sigma_z^2\mathbf{I}_N\right)^{-1}\mathbf{y}, \tag{5}$$

where $\mathbf{r}_{\boldsymbol{\eta}} = \mathbb{E}\left[x(\boldsymbol{\eta})\mathbf{x}\right] \in \mathcal{R}^{N\times 1}$, and $\mathbf{I}_N$ is an identity matrix.

With the optimum MMSE receiver given in (5), the MSE $\sigma_{\boldsymbol{\eta}}^2$ can be calculated as

$$\sigma_{\boldsymbol{\eta}}^2 = 1 - \mathbf{r}_{\boldsymbol{\eta}}^T\left(\mathbf{R}_{xx} + \frac{\delta\theta}{\gamma_0}\mathbf{I}_N\right)^{-1}\mathbf{r}_{\boldsymbol{\eta}}, \tag{6}$$

where $\gamma_0 = \frac{P_0}{\sigma_z^2}$ is the signal-to-noise ratio (SNR) per unit area. The MSE $\sigma_{\boldsymbol{\eta}}^2$ given in (6) is a function of $\boldsymbol{\eta}$, the SNR γ_0, the spatial correlation coefficient ρ_s, the temporal correlation coefficient ρ_t, the spatial node density δ, and the temporal sampling rate θ.

Given a fixed transmission power per unit area, a smaller node density and/or temporal sampling rate means more transmission energy per sample, thus a better SNR per sample, which can benefit the system performance. On the other hand, a smaller node density and/or sampling rate means less samples per unit area per unit time, thus a smaller correlation among the nodes, which can degrade the estimation performance.

In order to distinguish the opposite effects of the SNR per sample and the sample correlation, we can decompose the MMSE in (5) into two steps. The first step estimates the discrete data samples collected by the sensors, and the second step obtains an estimate of an arbitrary data point by interpolating the results from the first step. It is demonstrated in [14] that the two-step method is equivalent to the optimum estimation described in (5). We will investigate the performance of the two estimation steps in the next two sections, respectively.

III. MMSE Estimation of the Discrete Samples

The MMSE estimation of the discrete data samples collected by the sensors is discussed in this section.

A. Asymptotic Analysis

The FC obtains an estimate of the N discrete space-time samples, $\mathbf{x}$, with a linear MMSE receiver as

$$\hat{\mathbf{x}} = \mathbf{W}_x^T\mathbf{y}, \tag{7}$$

where $\hat{\mathbf{x}} \in \mathcal{C}^{N\times 1}$ is the MMSE estimate of $\mathbf{x}$. The MMSE matrix, $\mathbf{W}_x \in \mathcal{R}^{N\times N}$, needs to minimize the normalized MSE (NMSE), $\sigma_{st,N}^2 = \frac{1}{N}\mathbb{E}\|\hat{\mathbf{x}} - \mathbf{x}\|^2$, and can be solved through the orthogonal principal, $\mathbb{E}\left[(\hat{\mathbf{x}}_s - \mathbf{x})\mathbf{y}\right] = 0$. The result is

$$\mathbf{W}_x^T = \sqrt{E_{ij}}\mathbf{R}_{xx}\left(E_{ij}\mathbf{R}_{xx} + \sigma_z^2\mathbf{I}\right)^{-1}. \tag{8}$$

The error correlation matrix, $\mathbf{R}_{ee}^{(x)} = \mathbb{E}\left[\mathbf{e}_s\mathbf{e}_s^T\right]$, with $\mathbf{e}_s = \hat{\mathbf{x}} - \mathbf{x}$, can then be calculated as

$$\mathbf{R}_{ee}^{(x)}{=}\mathbf{R}_{xx}{-}\mathbf{R}_{xx}\left(\mathbf{R}_{xx}+\frac{\delta\theta}{\gamma_0}\mathbf{I}\right)^{-1}\mathbf{R}_{xx}{=}\left(\mathbf{R}_{xx}^{-1}{+}\frac{\gamma_0}{\delta\theta}\mathbf{I}_N\right)^{-1}, \quad (9)$$

where the orthogonal principal is used in the first equality, and the second equality is based on the identify $\mathbf{D}^{-1}+\mathbf{D}^{-1}\mathbf{C}(\mathbf{A}-\mathbf{B}\mathbf{D}^{-1}\mathbf{C})^{-1}\mathbf{B}\mathbf{D}^{-1} = (\mathbf{D}-\mathbf{C}\mathbf{A}^{-1}\mathbf{B})^{-1}$.

The NMSE can be calculated as $\sigma_{st,N}^2 = \frac{1}{N}\text{trace}\left(\mathbf{R}_{ee}^{(x)}\right)$, where trace$(\mathbf{A})$ returns the trace of the matrix $\mathbf{A}$. From (9), the calculation of the NMSE involves matrix inversion and the trace operation. In order to explicit identify the impacts of the node density and sampling rate on the NMSE, we resort to the asymptotic analysis as follows.

Proposition 1: Let $N_s \to \infty$ and $N_t \to \infty$ while keeping both δ and θ finite, the NMSE of the estimation of the discrete samples collected by the sensors is

$$\sigma_{st}^2 = \lim_{N\to\infty}\sigma_{st,N}^2 = \frac{\sqrt{2}}{\pi\sqrt{\beta}}\cdot K\left(\sqrt{\frac{\alpha}{\beta}}\right) \quad (10)$$

where $K(\cdot)$ is the complete elliptic integral of the first kind [11, eqn. (8.112.1)], and

$$\alpha = \frac{8\gamma_0}{\delta\theta}\cdot\frac{\rho_s^{\frac{1}{\delta}}}{1-\rho_s^{\frac{2}{\delta}}}\cdot\frac{\rho_t^{\frac{1}{\theta}}}{1-\rho_t^{\frac{2}{\theta}}}, \quad (11a)$$

$$\beta = \frac{1}{2}+\frac{\gamma_0}{\delta\theta}\left(1+\frac{2\rho_s^{\frac{2}{\delta}}}{1-\rho_s^{\frac{2}{\delta}}}\right)\left(1+\frac{2\rho_t^{\frac{2}{\theta}}}{1-\rho_t^{\frac{2}{\theta}}}\right)+\frac{1}{2}\left(\frac{\gamma_0}{\delta\theta}\right)^2+\frac{\alpha}{2}. \quad (11b)$$

Proof: Performing the eigenvalue decomposition of $\mathbf{R}_{xx}$ in (9), we can rewrite the NMSE as

$$\sigma_{st,N}^2 = \frac{1}{N}\sum_{m=1}^{N_s-1}\sum_{k=1}^{N_t-1}\left(\frac{1}{\lambda_{m,k}}+\frac{\gamma_0}{\delta\theta}\right)^{-1}, \quad (12)$$

where $\lambda_{m,k}$, for $m = 0, 1, \cdots, N_s-1$, and $k = 0, 1, \cdots, N_t-1$, are the eigenvalues of $\mathbf{R}_{xx}$. When $N_s \to \infty$ and $N_t \to \infty$, the 2D discrete-time Fourier transform (DTFT) of the sequence, $\left\{\rho_s^{|m|d}\rho_t^{|k|T_s}\right\}_{m,k}$, which are elements of the TBT matrix $\mathbf{R}_{xx}$, can be calculated as $\Lambda_{xx}(f_1, f_2) = \Lambda_s(f_1)\times\Lambda_t(f_2)$, with

$$\Lambda_s(f_1){=}\sum_{m=-\infty}^{+\infty}\rho_s^{|m|d}e^{-j2\pi(mf_1)}{=}\frac{1-\rho_s^{2d}}{1{+}\rho_s^{2d}{-}2\rho_s^d\cos(2\pi f_1)} \quad (13a)$$

$$\Lambda_t(f_2){=}\sum_{k=-\infty}^{+\infty}\rho_t^{|k|T_s}e^{-j2\pi(kf_2)}{=}\frac{1-\rho_t^{2T_s}}{1{+}\rho_t^{2T_s}{-}2\rho_t^{T_s}\cos(2\pi f_2)} \quad (13b)$$

Based on [9, Theorem 1], when $N_s{\to}\infty$ and $N_t{\to}\infty$, (12) can be rewritten as

$$\sigma_{st}^2{=}\lim_{N\to\infty}\sigma_{st,N}^2{=}\int_{-\frac{1}{2}}^{\frac{1}{2}}\int_{-\frac{1}{2}}^{\frac{1}{2}}\left[\frac{1}{\Lambda_{xx}(f_1,f_2)}+\frac{\gamma_0}{\delta\theta}\right]^{-1}df_1df_2, \quad (14)$$

Substituting the result of $\Lambda_{xx}(f_1, f_2)$ into (14), and applying the identity [11, eqn. (2.553.3)], we can solve the inner integral. Based on [11, eqn. (2.580.2)], [11, eqn. (3.152.2)], and simplifying, we can get the results in (10). ■

In Proposition 1, the spatial-temporal sampling affects the NMSE in the form of the following functions, $f_1(\delta){=}\frac{\rho_s^{\frac{2}{\delta}}}{1-\rho_s^{\frac{2}{\delta}}}$, $g_1(\delta){=}\frac{\rho_s^{\frac{1}{\delta}}}{1-\rho_s^{\frac{2}{\delta}}}$, $f_2(\theta){=}\frac{\rho_t^{\frac{2}{\theta}}}{1-\rho_t^{\frac{2}{\theta}}}$, $g_2(\theta){=}\frac{\rho_t^{\frac{1}{\theta}}}{1-\rho_t^{\frac{2}{\theta}}}$, and $f_3(\delta,\theta){=}\frac{\gamma_0}{\delta\theta}$. Among them, $f_1(\delta)$ and $g_1(\delta)$ are related to the spatial correlation, and they are increasing functions of δ. $f_2(\theta)$ and $g_2(\theta)$ are related to the temporal correlation, and they are increasing functions of θ. The function $f_3(\delta, \theta)$ represents the SNR per sample, and it is a decreasing function of both δ and θ.

In proposition 1, if we assume that the data is spatially correlated but temporally uncorrelated, then the NMSE of the spatial samples can be simplified as follows.

Corollary 1: If $\rho_t = 0$, the asymptotic NMSE of the estimation for the spatially correlated samples is

$$\sigma_s^2 = \left[\left(1+\frac{\gamma_0}{\delta\theta}\right)^2+\frac{4\gamma_0\rho_s^{\frac{2}{\delta}}}{\delta\theta\left(1-\rho_s^{\frac{2}{\delta}}\right)}\right]^{-\frac{1}{2}}. \quad (15)$$

Proof: Taking $\rho_t = 0$ leads to $\alpha = 0$ and $\beta = 0.5 + (1+2f_1(\delta))f_3(\delta)+0.5f_3(\delta,\theta)^2$. Eqn. (15) can be obtained by substituting β into (10). ■

The result in Corollary 1 coincides with [2, eqn. (12)], where only the spatial samples are considered. It was shown in [2] analytically that σ_s^2 is an increasing function in δ.

Based on the symmetry between the space and time domains, a similar result can be obtained for the estimation of spatially uncorrelated but temporally correlated data, by exchanging ρ_s with ρ_t, and δ with θ in (15).

B. Properties of Spatial-Temporal Sampling

Fig. 2 shows the asymptotic NMSE of the data samples as a function of the node density δ and the temporal sampling rate θ with $\rho_s = \rho_t = 0.3$ and $\gamma_0 = 10$ dB. It can be seen from the figure that the NMSE is an increasing function of δ and θ. This indicates the NMSE for estimating discrete data samples can benefit from a smaller spatial-temporal sampling rate. Therefore, if we only want to obtain the data at some discrete time and locations, we should use a node density and sampling rate that are as small as allowed by the application.

In addition, when both $\theta \to \infty$ and $\delta \to \infty$, it is discovered that the NMSE is upper bounded in both the space and time domains, as stated in the following corollary.

Corollary 2: For the estimation of the data samples, the asymptotic NMSE is upper bounded by

$$\sigma_{st}^2 \le \frac{2}{\pi}\left\{1+4\gamma_0/\left[\log(\rho_s)\log(\rho_t)\right]\right\}^{-\frac{1}{2}}\cdot K(\Delta_{\delta r}), \quad (16)$$

with $\Delta_{\delta r} = \left\{4\gamma_0/\left[4\gamma_0+\log(\rho_s)\log(\rho_t)\right]\right\}^{\frac{1}{2}}$.

Proof: Eqn. (16) can be directly proved by letting $\lim_{\delta\to\infty,\theta\to\infty}\sigma_{st}^2$ in (10). ■

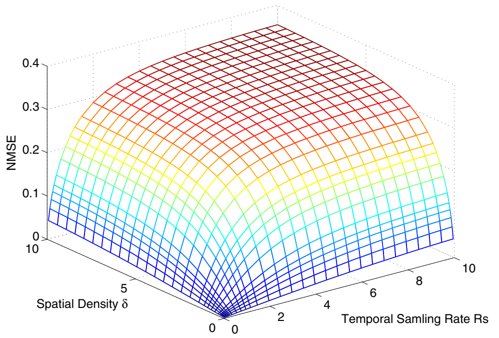

Fig. 2. The asymptotic NMSE for the estimation of discrete samples.

IV. MMSE Spatial-Temporal Interpolation

This section discusses the performance of space-time interpolation, *i.e.*, the estimation of any arbitrary point on the 2D space-time plane by interpolating the N discrete samples.

A. Space-Time Interpolation

Since we are interested in the reconstruction fidelity of the entire space-time plane, the worst case scenario is considered by estimating the data located in the middle of the square formed by four adjacent samples, with the coordinates of the data points to be estimated being $x'_{ij} = x[(i+\frac{1}{2})d, (j+\frac{1}{2})T_s]$, for $i = 0, \cdots, N_s - 1$ and $j = 0, \cdots, N_t - 1$. Define the interpolation data vector as $\boldsymbol{\xi} = \left[\mathbf{x}_0'^T, \cdots, \mathbf{x}_{(N_s-1)}'^T\right]^T \in \mathcal{R}^{N\times 1}$, where $\mathbf{x}'_i = \left[x'_{i0}, x'_{i1}, \cdots, x'_{i(N_t-1)}\right]^T \in \mathcal{R}^{N_t \times 1}$.

The FC obtains an estimate of $\boldsymbol{\xi}$ by interpolating the discrete samples with the MMSE criterion, $\hat{\boldsymbol{\xi}} = \mathbf{W}_{\xi}^T \mathbf{y}$, where $\mathbf{W}_\xi \in \mathcal{R}^{N\times N}$ is designed to minimize the NMSE $\vartheta^2_{st,N} = \frac{1}{N}\mathbb{E}\|\hat{\boldsymbol{\xi}} - \boldsymbol{\xi}\|^2$. Based on the orthogonal principal, $\mathbb{E}\left[(\hat{\boldsymbol{\xi}} - \boldsymbol{\xi})\mathbf{y}^T\right] = \mathbf{0}$, the MMSE space-time interpolations can be expressed by

$$\hat{\boldsymbol{\xi}} = \sqrt{E_{ij}}\mathbf{R}_{\xi x}\left(E_{ij}\mathbf{R}_{xx} + \sigma_z^2 \mathbf{I}\right)^{-1}\mathbf{y}, \tag{17}$$

with $\mathbf{R}_{\xi x} \triangleq \mathbb{E}(\boldsymbol{\xi}\mathbf{x}) = \mathbf{R}'_s \otimes \mathbf{R}'_t$ being a TBT matrix. The matrix $\mathbf{R}'_s$ is a Toeplitz matrix with the first row being $\rho_s^{\frac{d}{2}}[1, 1, \rho_s^d, \cdots, \rho_s^{(N_s-2)d|}]^T \in \mathcal{R}^{N_s\times 1}$, and the first column $\rho_s^{\frac{d}{2}}[1, \rho_s^d, \cdots, \rho_s^{(N_s-1)d|}]^T \in \mathcal{R}^{N_s \times 1}$. Similarly $\mathbf{R}'_t$ can be obtained by exchanging ρ_s with ρ_t and d with T_s in $\mathbf{R}'_s$. The error correlation matrix, $\mathbf{R}_{ee}^{(\xi)} \triangleq \mathbb{E}\left[(\hat{\boldsymbol{\xi}} - \boldsymbol{\xi})(\hat{\boldsymbol{\xi}} - \boldsymbol{\xi})^T\right]$, can then be calculated by

$$\mathbf{R}_{ee}^{(\xi)} = \mathbf{R}_{xx} - \mathbf{R}_{\xi x}\left(\mathbf{R}_{xx} + \frac{\theta\delta}{\gamma_0}\mathbf{I}_N\right)^{-1}\mathbf{R}_{x\xi}, \tag{18}$$

where $\mathbf{R}_{\xi\xi} = \mathbb{E}(\boldsymbol{\xi}\boldsymbol{\xi}^T) = \mathbf{R}_{xx}$ and $\mathbf{R}_{x\xi} = \mathbf{R}_{\xi x}^T$.

The relationship between the NMSE, $\vartheta^2_{st,N} = \frac{1}{N}\text{trace}\left(\mathbf{R}_{ee}^{(\xi)}\right)$, and the spatial-temporal sampling rates, δ and θ, is given in the following proposition.

Proposition 2: Let $N_s \to \infty$ and $N_t \to \infty$ while keeping both δ and θ finite, the asymptotic NMSE, $\vartheta^2_{st} \triangleq \lim_{N\to\infty}\vartheta^2_{st,N}$, of the spatial-temporal interpolation is

$$\vartheta^2_{st} = \frac{1-\rho_t^{\frac{1}{\theta}}}{1+\rho_t^{\frac{1}{\theta}}}\left\{1 + \int_{-\frac{1}{2}}^{\frac{1}{2}}\frac{1+\cos(2\pi f)}{v-\cos(2\pi f)}\left[\frac{q-\cos(2\pi f)}{p-\cos(2\pi f)}\right]^{\frac{1}{2}} df\right\} \tag{19}$$

where

$$v = \frac{1+\rho_t^{\frac{2}{\theta}}}{2\rho_t^{\frac{1}{\theta}}}, p = v + \frac{\gamma_0}{2\delta\theta}\frac{1-\rho_t^{\frac{2}{\theta}}}{\rho_t^{\frac{1}{\theta}}}\frac{1+\rho_s^{\frac{1}{\delta}}}{1-\rho_s^{\frac{1}{\delta}}}, q = v + \frac{\gamma_0}{2\delta\theta}\frac{1-\rho_t^{\frac{2}{\theta}}}{\rho_t^{\frac{1}{\theta}}}\frac{1-\rho_s^{\frac{1}{\delta}}}{1+\rho_s^{\frac{1}{\delta}}} \tag{20}$$

Proof: When $N_s \to \infty$ and $N_t \to \infty$, The 2D DTFT of the sequence, $\left\{\rho_s^{|m+\frac{1}{2}|d}\rho_t^{|k+\frac{1}{2}|T_s}\right\}_{m,k}$, which are elements of the TBT matrix $\mathbf{R}_{\xi x}$, can be calculated as $\Lambda_{\xi x}(f_1, f_2) = \Lambda'_s(f_1) \times \Lambda'_t(f_2)$, with

$$\Lambda'_s(f_1) = \rho_s^{\frac{d}{2}}\frac{(1-\rho_s^d)(1+e^{j2\pi f_1})}{1+\rho_s^{2d} - 2\rho_s^d\cos(2\pi f_1)}. \tag{21}$$

Similarly, $\Lambda'_t(f_2)$ can be obtained by exchanging ρ_s with ρ_t, and d with T_s in (21). Based on [9, Lemma 1], $\mathbf{R}_{\xi x}$ is asymptotically equivalent to a circulant-block-circulant (CBC) matrix, $\mathbf{C}_{\xi x} = \mathbf{U}_N^H\mathbf{D}_{\xi x}\mathbf{U}_N$, where $\mathbf{U}_N^H$ is the unitary discrete Fourier transform (DFT) matrix and $\mathbf{D}_{\xi x}$ is a diagonal matrix with its k-th diagonal element being $(\mathbf{D}_{\xi x})_{k,k} = \Lambda'_s\left(\frac{k-1}{N_s}\right)\cdot\Lambda'_t\left(\frac{k-1}{N_t}\right)$. Similarly, the TBT matrix, $\mathbf{R}_{xx}$, is asymptotically equivalent to a CBC matrix, $\mathbf{C}_{xx} = \mathbf{U}_N^H\mathbf{D}_{xx}\mathbf{U}_N$, where $(\mathbf{D}_{xx})_{k,k} = \Lambda_s\left(\frac{k-1}{N_s}\right)\cdot\Lambda_t\left(\frac{k-1}{N_t}\right)$, with $\Lambda_s(f_1)$ and $\Lambda_t(f_2)$ defined in (13).

From [12, Theorem 2.1], the error correlation matrix, $\mathbf{R}_{ee}^{(\xi)}$, is asymptotically equivalent to a CBC matrix, $\mathbf{C}_{ee}^{(\xi)} = \mathbf{C}_{xx} - \mathbf{C}_{\xi x}\left(\mathbf{C}_{xx} + \frac{\theta\delta}{\gamma_0}\mathbf{I}\right)^{-1}\mathbf{C}_{\xi x}^H = \mathbf{U}_N^H\mathbf{D}_{ee}^{(\xi)}\mathbf{U}_N$, where the diagonal matrix $\mathbf{D}_{ee}^{(\xi)} = \mathbf{D}_{xx} - \mathbf{D}_{\xi x}\left(\mathbf{D}_{xx} + \frac{\theta\delta}{\gamma_0}\mathbf{I}\right)^{-1}\mathbf{D}_{\xi x}^H$.

Based on the extension of the Szego's theorem to TBT matrices [9, Theorem 1], we have

$$\vartheta^2_{st} = \int_{-\frac{1}{2}}^{\frac{1}{2}}\int_{-\frac{1}{2}}^{\frac{1}{2}}\left[\Lambda_{xx}(f_1, f_2) - \frac{|\Lambda_{\xi x}(f_1, f_2)|^2}{\Lambda_{xx}(f_1, f_2) + \frac{\theta\delta}{\gamma_0}}\right] df_1 df_2. \tag{22}$$

With [11, eqn. (2.559.2)] and [11, eqn. (2.558.2)], we can solve the inner integral and (19) follows. ■

The results in Proposition 2 illustrate the asymptotic NMSE performance for the MMSE interpolation in both the space and time domains. The integrand in (19) is composed for elementary functions, and the integration limit is finite. Therefore the integral can be easily evaluated numerically.

If we assume the data samples are temporally uncorrelated ($\rho_t = 0$), and perform the interpolation only in the space domain based on the spatially correlated data samples, the NMSE given in (19) can be simplified as follows.

Corollary 3: If $\rho_t = 0$, the asymptotic NMSE of the estimation for the spatial interpolation is

$$\vartheta^2_s = \left(\frac{\delta\theta}{\gamma_0} + \frac{1-\rho_s^{\frac{1}{\delta}}}{1+\rho_s^{\frac{1}{\delta}}}\right)^{\frac{1}{2}}\left(\frac{\delta\theta}{\gamma_0} + \frac{1+\rho_s^{\frac{1}{\delta}}}{1-\rho_s^{\frac{1}{\delta}}}\right)^{-\frac{1}{2}} \tag{23}$$

Proof: When $\rho_t = 0$, we have $\Lambda_t(f_2) = 1$. Substituting $\Lambda'_t(f_2) = \Lambda_t(f_2) = 1$ into (22) and applying [11, eqn. (2.559.2)], we have (23). ■

The result in Corollary 3 simplifies to [14, Proposition 2]. It was demonstrated in [14] that the NMSE in (23) is a decreasing

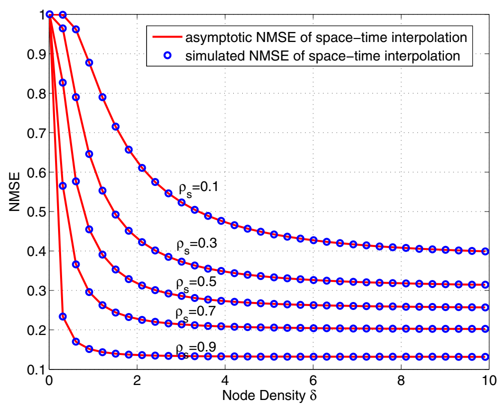

Fig. 3. The asymptotic NMSE for the space-time interpolation.

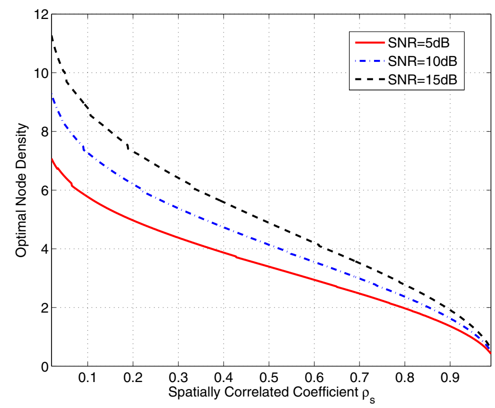

Fig. 4. The spatial optimal node density v.s. spatial correlation coefficient ρ_s.

function of the node density δ. With the symmetry between the space and time domains, we can get a similar result for the interpolation of spatially uncorrelated but temporally correlated data samples.

B. Optimum Spatial-Temporal Sampling

Fig. 3 shows the asymptotic NMSE as a function of the node density, δ, under various values of ρ_s. In the simulation, we have $\gamma_0 = 10$ dB, $\rho_t = 0.5$, and $\theta = 10$. In the simulation, $N_s = N_t = 60$ samples are used to approximate infinite number of samples. Excellent match is observed between the simulation results the asymptotic results. Different from the results in Fig. 2, the NMSE of the space-time interpolation is a decreasing function of δ and θ. This can be intuitively explained by the fact that the interpolation depends mainly on the spatial-temporal correlation among the data samples, and a higher space-time sampling rate means a stronger correlation, thus a better estimation fidelity.

It also can be seen from Fig. 3 that, when δ is small, the MSE decreases dramatically as δ increases. When δ reaches a certain threshold, no apparent performance gain can be achieved by increasing δ further, *i.e.*, the slope of ϑ_{st}^2 approaches zero as δ increase. Thus, we can find the optimum node density by solving the equation $\left|\frac{\partial \vartheta_{st}^2}{\partial \delta}\right|_{\delta_0} = \epsilon_s$, with ϵ_s being a small number.

Fig. 4 shows the optimum node density as a function of the spatial correlation coefficient, under the value of $\rho_t = 0$. The value of $\epsilon_s = 10^{-5}$ is used in the figure. The results in this figure demonstrate that the optimum node density decreases as ρ_s increases. Therefore, for the estimation of the spatial interpolation, a smaller node density is required for a field with a stronger spatial correlation. Due to the space-time symmetry, a similar result is observed for the optimum sampling rate, and details are omitted here for brevity.

V. Conclusions

In this paper, the optimum sampling in a WSN with spatial-temporally correlated data was studied. The impacts of the spatial-temporal sampling on the NMSE of the data reconstructed at the FC were investigated through asymptotic analysis, where the number of samples tends to infinity while both the spatial node density and the temporal sampling rate remain constant. Exact analytical expressions of the asymptotic NMSE were obtained under the constraint of fixed power per unit area.

There were two observations. First, if the network only needs to estimate the discrete samples, the NMSE is an increasing function of the node density or the sampling rate. Second, for the estimation of an arbitrary point on the 2D space-time plane, the NMSE is a decreasing function of the node density or the sampling rate, and the optimum sampling rate can be found when the MSE-rate slope is close to zero.

References

[1] Y. Sung, H. V. Poor, and H. Yu, "Optimal node density for two-dimensional sensor arrays," in *Proc. IEEE Sensor Array Multichannel Signal Processing Workshop*, pp. 271-274, 2008.

[2] J. Wu and N. Sun, "Optimal sensor density in a distortion-tolerant linear wireless sensor network," in *Proc. IEEE Global Telecommun. Conf. GLOBECOM'10*, Dec. 2010.

[3] J. F. Chamberland and V. V. Veeravalli, "How dense should a sensor network be for detection with correlated observations?" *IEEE Trans. Information theory*, vol. 52, pp. 5099-5106, Nov. 2006.

[4] M. C. Vuran, O. B. Akan, and I. F. Akyildiz, Spatio-Temporal Correlation: Theory and Applications for Wireless Sensor Networks, Computer Networks Journal (Elsevier), vol. 45, pp. 245-261, Jun. 2004.

[5] R. Cristescu and M. Vetterli, "On the optimal density for real-time data gathering of spatio-temporal processes in sensor networks," *IEEE Trans. Signal Processing*, vol. 51, pp. 159-164, Aug. 2003.

[6] X. Zhang, H. Wang, F. N. Abdesselam, and A. A. Khokhar, "Distortion Analysis for Real-Time Data Collection of Spatially Temporally Correlated Data Fields in Wireless Sensor Networks," *IEEE Trans. Vehicular Technology*, vol. 58, pp. 1583-1594, Mar. 2009.

[7] S. Bandyopadhyay, Q. Tian, and E. J. Coyle, "Spatio-Temporal Sampling Rates and Energy Efficiency in Wireless Sensor Networks," *IEEE Trans. Networking*, vol. 13, pp. 1339-1352, Dec. 2005

[8] M. Gastpar and M. Vetterli, "Power, Spatio-Temporal Bandwidth, and Distortion in Large Sensor Networks," *IEEE Journal On Selected Areas In Commun.*, vol. 23, pp. 745-755, Apr. 2005.

[9] P. A. Voois, "A theorem on the asymtotic eigenvalue distribution of Toeplitz-block-Toeplitz matrix," *IEEE Trans. Signal Processing*, vol. 44, pp. 1837-1841, July 1996.

[10] S. M. Kay, *Fundamentals of Statistical Signal Processing, vol. I, Estimation Theory*, NJ: Prentice-Hall, 1993.

[11] I. S. Gradshteyn and I. M. Ryzhik, *Table of Integrals, Series, and Products*, 6nd ed. Academic Press, July 2000.

[12] R. M. Gray, Toeplitz and Circulant Matrices: A Review, NOW Publishers, 2006 (available online at http://ee.stanford.edu/ gray/).

[13] T. E Mazancourt and D. Gerlic, "The inverse of a block-circulant matrix," *IEEE Trans. Antennas and Propagation*, vol. AP-31, pp. 808-810, Sept. 1983.

[14] J. Wu and N. Sun, "Optimal sensor density in distortion-tolerant wireless sensor networks," submitted to *IEEE Trans. Wireless Commun.*, Jan. 2011.